WSRC-STI-2007-00414

SRNL
SAVANNAH RIVER NATIONAL LABORATORY

Stress Corrosion Cracking Susceptibility of High Level Waste Tanks during Sludge Mass Reduction

K. H. Subramanian

Savannah River National Laboratory
Materials Science and Technology Directorate

Publication Date: October 2007

Washington Savannah River Company
Savannah River Site
Aiken SC 29808

This document was prepared in connection with work done under Contract No. DE-AC09-96SR18500 with the U. S. Department of Energy

DISCLAIMER

DOCUMENT: WSRC-STI-2007-00414

TITLE: Stress Corrosion Cracking Susceptibility of High Level Waste Tanks during Sludge Mass Reduction

APPROVALS

APPROVAL SIGNATURES ON FILE

Table of Contents

1 SUMMARY 1

2 INTRODUCTION 1

3 BACKGROUND 3

4 TECHNICAL APPROACH 5

4.1 ELECTROCHEMICAL TESTING: ANODIC POLARIZATION 5
4.2 MATRIX 6
4.3 MECHANICAL TESTING 7

5 ELECTROCHEMICAL TEST RESULTS 7

5.1 ANODIC POLARIZATION SCANS: 5M/10M NAOH + $NaNO_3$ 7
5.2 ANODIC POLARIZATION SCANS: 5M/10M NAOH + 0.1M$NaNO_3$ + $NaAlO_2$ 10
5.3 ANODIC POLARIZATION SCANS: 5M/10M NAOH + 0.5M$NaNO_3$ + $NaAlO_2$ 13
5.4 ANODIC POLARIZATION SCANS: 5M/10M NAOH +1.0M$NaNO_3$ + $NaAlO_2$ 16

6 ELECTROCHEMICAL TEST DISCUSSION 19

7 RESULTS OF MECHANICAL TESTING 21

8 CONCLUSION 25

REFERENCES 26

List of Tables

TABLE 1: RECOMMENDED CHEMISTRY CONTROL ENVELOPE DURING SLUDGE MASS REDUCTION 1
TABLE 2: TEMPERATURE LIMITS FOR NON-SLURRIED WASTE TANKS WITH NITRATE CONCENTRATIONS LESS THAN 1M.....3
TABLE 3: TEMPERATURE LIMITS FOR SLURRIED WASTE TANKS WITH NITRATE CONCENTRATIONS LESS THAN 1M 3
TABLE 4: NOMINAL COMPOSITION OF ASTM A516-70 STEEL.....6
TABLE 5: TEST MATRIX VARIABLES (PARAMETRIC MATRIX).....6
TABLE 6: RESULTS OF DYE PENETRANT TESTING 22
TABLE 7: RECOMMENDED CHEMISTRY CONTROL ENVELOPE DURING SLUDGE MASS REDUCTION 25

List of Figures

FIGURE 1: CAUSTIC STRESS CORROSION CRACKING SERVICE GRAPH [] 2
FIGURE 2: SCHEMATIC OF ANODIC POLARIZATION CURVE SHOWING ZONES SUSCEPTIBLE TO SCC [] 6
FIGURE 3: U-BEND COUPONS 7
FIGURE 4: ANODIC POLARIZATION IN 5M NAOH WITH ADDITIONS OF $NaNO_3$ AT 95C.....8
FIGURE 5:ANODIC POLARIZATION IN 5M NAOH WITH ADDITIONS OF $NaNO_3$ AT 105C.....9
FIGURE 6: ANODIC POLARIZATION IN 5M NAOH WITH ADDITIONS OF $NaNO_3$ AT 95°C 9
FIGURE 7: ANODIC POLARIZATION SCAN IN 5M NAOH WITH 0.1M $NaNO_3$ AND ADDITIONS OF $NaAlO_2$ AT 95°C 10
FIGURE 8: ANODIC POLARIZATION SCAN IN 5M NAOH WITH 0.1M $NaNO_3$ AND ADDITIONS OF $NaAlO_2$ AT 105°C ..11
FIGURE 9:ANODIC POLARIZATION SCAN IN 10M NAOH WITH 0.1M $NaNO_3$ AND ADDITIONS OF $NaAlO_2$ AT 95°C ...12
FIGURE 10: ANODIC POLARIZATION SCAN IN 10M NAOH WITH 0.1M $NaNO_3$ AND ADDITIONS OF $NaAlO_2$ AT 105°C 12
FIGURE 11: ANODIC POLARIZATION SCAN IN 5M NAOH WITH 0.5M $NaNO_3$ AND ADDITIONS OF $NaAlO_2$ AT 95°C ..13
FIGURE 12: ANODIC POLARIZATION SCAN IN 5M NAOH WITH 0.5M $NaNO_3$ AND ADDITIONS OF $NaAlO_2$ AT 105°C 14
FIGURE 13: ANODIC POLARIZATION SCAN IN 10M NAOH WITH 0.5M $NaNO_3$ AND ADDITIONS OF $NaAlO_2$ AT 95°C 15
FIGURE 14: ANODIC POLARIZATION SCAN IN 10M NAOH WITH 0.5M $NaNO_3$ AND ADDITIONS OF $NaAlO_2$ AT 105°C 15
FIGURE 15: ANODIC POLARIZATION SCAN IN 5M NAOH WITH 1M $NaNO_3$ AND ADDITIONS OF $NaAlO_2$ AT 95°C 16
FIGURE 16: ANODIC POLARIZATION SCAN IN 5M NAOH WITH 1M $NaNO_3$ AND ADDITIONS OF $NaAlO_2$ AT 105°C ...17
FIGURE 17: ANODIC POLARIZATION SCAN IN 10M NAOH WITH 1M $NaNO_3$ AND ADDITIONS OF $NaAlO_2$ AT 95°C ...18
FIGURE 18:ANODIC POLARIZATION SCAN IN 10M NAOH WITH 1M $NaNO_3$ AND ADDITIONS OF $NaAlO_2$ AT 105°C ..18
FIGURE 19: EFFECT OF $NaNO_3$ ADDITION TO NAOH SOLUTIONS ON E_{OC}. 19
FIGURE 20: E_{OC} AS A FUNCTION OF ALUMINATE IN 0.1M NaNO3/NAOH SOLUTIONS 20
FIGURE 21: E_{OC} AS A FUNCTION OF ALUMINATE IN 0.5M $NaNO_3$/NAOH SOLUTIONS. 20
FIGURE 22: E_{OC} AS A FUNCTION OF ALUMINATE IN 1M $NaNO_3$/NAOH SOLUTIONS 21
FIGURE 23: U-BEND COUPONS IN TEST 22

.

1 SUMMARY

Aluminum is a principal element in alkaline nuclear sludge waste stored in high level waste (HLW) tanks at the Savannah River Site. The mass of sludge in a HLW tank can be reduced through the caustic leaching of aluminum, i.e. converting aluminum oxides (gibbsite) and oxide-hydroxides (boehmite) into soluble hydroxides through reaction with a hot caustic solution. The temperature limits outlined by the chemistry control program for HLW tanks to prevent caustic stress corrosion cracking (CSCC) in concentrated hydroxide solutions will potentially be exceeded during the sludge mass reduction (SMR) campaign. Corrosion testing was performed to determine the potential for CSCC under expected conditions.

The experimental test program, developed based upon previous test results and expected conditions during the current SMR campaign, consisted of electrochemical and mechanical testing to determine the susceptibility of ASTM A516 carbon steel to CSCC in the relevant environment. Anodic polarization test results indicated that anodic inhibition at the temperatures and concentrations of interest for SMR is not a viable, consistent technical basis for preventing CSCC. However, the mechanical testing concluded that CSCC will not occur under conditions expected during SMR for a minimum of 35 days. In addition, the stress relief for the Type III/IIIA tanks adds a level of conservatism to the estimates.

The envelope for corrosion control is recommended during the SMR campaign is shown in Table 1. The underlying assumption is that solution time-in-tank is limited to the SMR campaign. The envelope recommends nitrate/aluminate intervals for discrete intervals of hydroxide concentrations, although it is recognized that a continuous interval may be developed. The limits also sets temperature limits.

Table 1: Recommended Chemistry Control Envelope During Sludge Mass Reduction

Hydroxide Concentration (M)	Nitrate Concentration (M)	Aluminate Concentration (M)	Temperature (°C)
$[OH^-] < 5$	$0.2 < [NO_3^-] \leq 1$	$[AlO_2^-] \leq 1$	105°C
$5 \leq [OH^-] \leq 10$	$0.5 < [NO_3^-] \leq 1$	$[AlO_2^-] \leq 1$	105°C

Further U-bend testing is recommended under polarized conditions to determine whether the mechanical conditions exist for SCC when the test is electrochemical biased towards initiating CSCC.

2 INTRODUCTION

Aluminum is a principal element in alkaline nuclear sludge waste stored in high level waste (HLW) tanks at the Savannah River Site. The mass of sludge in a HLW tank can be reduced through the caustic leaching of aluminum, i.e. converting aluminum oxides (gibbsite) and oxide-hydroxides (boehmite) into soluble hydroxides through reaction with a hot caustic solution. The process chemistry, similar to the Bayer process in the aluminum industry, nominally follows the reactions:

$$Al(OH)_3(gibbsite) + NaOH \rightarrow NaAlO_{2(soluble)} + 2H_2O$$
$$AlO \bullet OH(boehmite) + NaOH \rightarrow NaAlO_{2(soluble)} + H_2O$$

The aluminum dissolution is done by introducing hot caustic solution (the temperature and concentration will be defined per the specific chemistry of the tank) and slurrying to ensure mixing. The high level waste tanks are potentially susceptible to stress corrosion cracking under exposure to these highly caustic solutions at high temperatures, known as 'caustic stress corrosion cracking' (CSCC). The caustic soda service graph (shown in Figure 1) is a compilation of the recommended usage for materials for use with high hydroxide solutions. The caustic soda service graph is a compilation of data available regarding stress corrosion cracking in a variety of concentrated sodium hydroxide solutions over a range of temperature. The graph indicates that for exposure to 30% (approximately 10M) NaOH by weight, the acceptable regime of use for low carbon steel with stress relieved welds is below 100°C (Area 'B') with the mid-point of this regime at approximately 80°C. The service graph recommends that within the susceptible region, the welds be stress-relieved. The stress-relief of the Type III/IIIA tanks are

expected to prevent all forms of stress corrosion cracking, but chemistry controls are followed for additional conservatism in their operations.

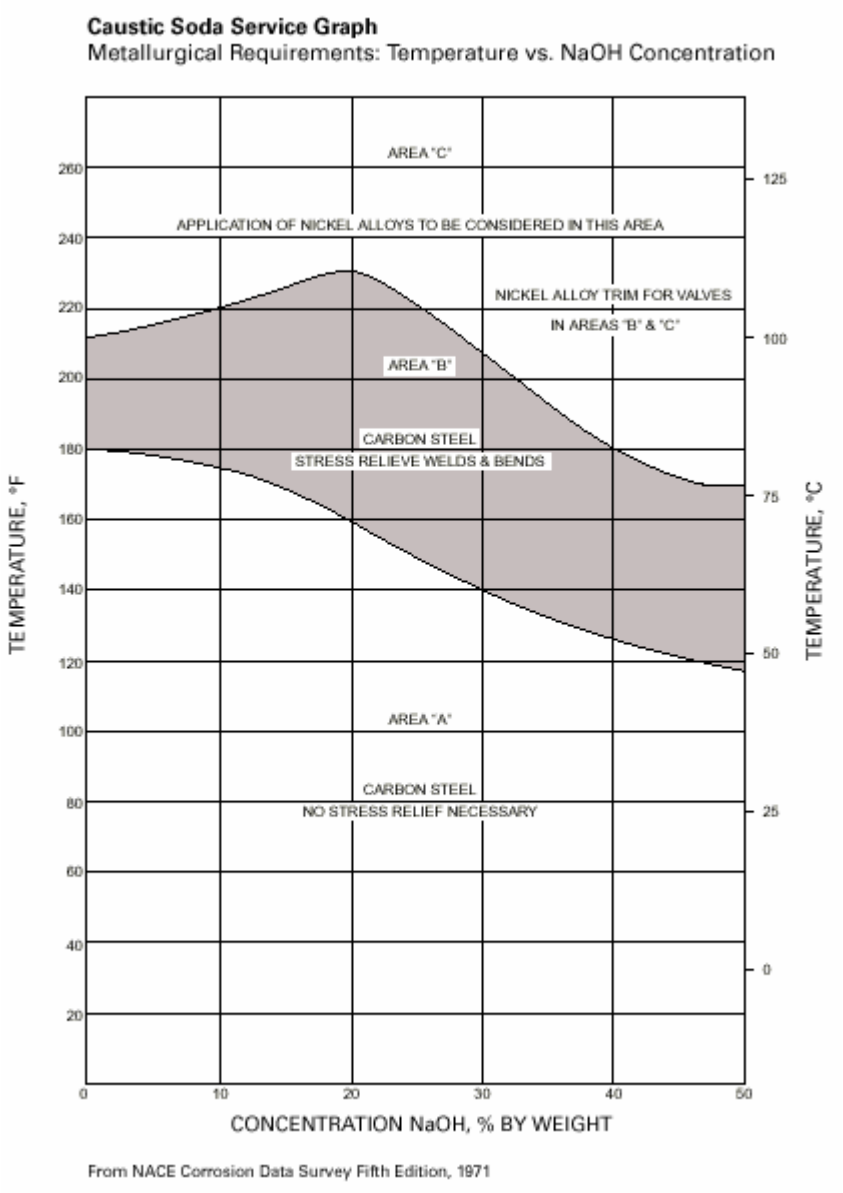

Figure 1: Caustic Stress Corrosion Cracking Service Graph [1]

.

The current chemistry control program places temperature limits, as shown in Table 2 and 3, on solutions containing low levels of nitrate (expected to prevent CSCC) when hydroxide is present.[2] The slurried tanks have higher temperature limits under the assumption of complete mixing.

Table 2: Temperature Limits for Non-Slurried Waste Tanks with Nitrate Concentrations Less than 1M

Supernate Concentration	$T_{supernate}$		T_{ss}/T_w*	
Hydroxide (M)	**$[NO_3^-] \leq 0.02M$**	**$0.02M < [NO_3^-] \leq 1M$**	**$[NO_3^-] \leq 0.02M$**	**$0.02M < [NO_3^-] \leq 1M$**
$0.01 < [OH^-] \leq 1$	40°C	40°C	T_{ss} = 75°C T_w = 70°C	T_{ss} = 75°C T_w = 70°C
$1 < [OH^-] \leq 8$	60°C	100°C	T_{ss} = 60°C T_w = 55°C	T_{ss} = 100°C T_w = 95°C
$[OH^-] > 8$	60°C	60°C	T_{ss} = 60°C T_w = 55°C	T_{ss} = 60°C T_w = 55°C

*T_{ss} = Temperature of salt or sludge phase
T_w = Temperature of tank wall

Table 3: Temperature Limits for Slurried Waste Tanks with Nitrate Concentrations Less than 1M

Supernate Concentration	$T_{supernate}$		T_{ss}/T_w*	
Hydroxide (M)	**$[NO_3^-] \leq 0.02M$**	**$0.02M < [NO_3^-] \leq 1M$**	**$[NO_3^-] \leq 0.02M$**	**$0.02M < [NO_3^-] \leq 1M$**
$0.01 < [OH^-] \leq 1$	75°C	75°C	T_{ss} = 75°C T_w = 70°C	T_{ss} = 75°C T_w = 70°C
$1 < [OH^-] \leq 8$	60°C	100°C	T_{ss} = 60°C T_w = 55°C	T_{ss} = 100°C T_w = 95°C
$[OH^-] > 8$	60°C	60°C	T_{ss} = 60°C T_w = 55°C	T_{ss} = 60°C T_w = 55°C

*T_{ss} = Temperature of salt or sludge phase
T_w = Temperature of tank wall

The temperature limits for high hydroxide solutions will be exceeded during sludge mass reduction and corrosion testing was performed to determine the potential for CSCC under expected conditions, which include solutions with nitrate/aluminate additions.

3 BACKGROUND

Stress corrosion cracking is due to the combined action of a corrosive medium and tensile stresses on a material causing cracking at lower stresses than dry cracking. The CSCC of low carbon steels has been studied for over 50 years and several review papers have been published summarizing the effects of various metallurgical and environmental factors that contribute to stress corrosion cracking susceptibility of mild steel in alkaline solutions.[3,4] The minimum concentration of hydroxide required to produce CSCC is reported to be 5% NaOH and the greatest susceptibility to SCC has been correlated with electrochemical potentials observed for the transition from a passive to active condition. In 10M NaOH, the transition is reported to begin at approximately -1.0 V-SCE and is manifested as an anodic peak on an anodic polarization curve.[3] However, the critical potentials at which cracking is most evident is reported to be dependent upon steel composition, most notably carbon composition.[5] Additionally, the current densities correlating to critical potentials that are observed are subject to change under strain.[6]

The use of inhibitors to prevent CSCC has also been the focus of much research. There is contradictory evidence on the efficacy of nitrate as an inhibitor that has led to it being deemed an "unsafe inhibitor".[7] Small additions of sodium nitrate to hydroxide solution have been reported to cause cracking, where pure NaOH did not produce

failure.[8] Additionally, it has been reported that bubbling oxygen through a boiling NaOH solution prevented cracking, as did nitrogen. These dissolved gases are proposed to affect the formation of the passive film, and consequently the onset of SCC.

Several SRS experimental programs, focused on the HLW tanks, concluded that CSCC was not an issue during alumina dissolution based upon slow-strain rate testing and threshold stress intensity testing performed on wedge-opening loaded specimens.* The testing was performed by exposing the test coupons to solutions within the following variable ranges[9,10]:

Temperature	60 - 100°C
[NaOH]	3.0 - 8.0 M
[$NaNO_3$]	0.2 - 2.0 M
[$NaNO_2$]	0.005 – 0.5 M
[$NaAlO_2$]	0.0 - 1.0 M

A more recent study to broaden the chemistry envelope, specifically to raise the temperature limits for hydroxide concentrations greater than 8M, undertook a systematic study to develop a fundamental understanding of the mechanisms by which to control CSCC with nitrate additions and temperature limits by determining the electrochemical conditions under which CSCC was promoted or controlled. The electrochemical testing consisted of anodic polarization scans to determine electrochemical potential regimes within which CSCC is possible. The results, confirmed with slow-strain rate testing, indicated that the active-passive transition peak seen in 10M NaOH, typically associated with CSCC at -0.25 V-SCE and –0.75V-SCE is still present with small and higher additions of nitrate.[11,12] However, there is a mid-range of nitrate concentrations within which the peak is not present and the magnitude of which is affected by temperature. The data suggested that the combination of dissolved oxygen and nitrate ensured a stable oxide on the surface, thereby reducing the propensity for CSCC. However, at lower concentrations of nitrate, the steel was not sufficiently polarized beyond the active-passive transitions. The lack of dissolved oxygen at higher temperatures does not sufficiently polarize the sample. Highly concentrated salt solutions, as a analogy to high temperature exposure, also insufficiently polarize the sample due to the high ionic strength and consequent low oxygen content. It was recommended, based upon the experimental results, that the temperature limits for hydroxide concentrations of greater than 8M NaOH, and less than 1M $NaNO_3$ be increased to 85°C, with a minimum of 0.5M $NaNO_3$ and a new chemistry control interval constructed between 0.5M $NaNO_3$ and 1M $NaNO_3$. [13]

The addition of aluminate ions to concentrated hydroxide solutions has been studied in reference to the aluminum process industry. The literature regarding the inhibiting effect of aluminate in hydroxide solutions is also somewhat contradictory. Literature data indicates that the aluminate ions may inhibit the anodic dissolution through the formation of a amorphous film containing the aluminate anion as opposed to the typical iron hydroxide that is adsorbed.[14] The typical iron hydroxide crystalline phase is soluble in the active region, and increases the peak current density prior to the active passive transition peak. However, with the competitive aluminate adsorption reaction, the iron hydroxide formation is proposed to retard the iron hydroxide formation. It has also been proposed that the formation of an amorphous (non-crystalline) films are beneficial to maintaining passivity. The competing adsorption reactions can be written as follows:

$$Fe + OH^- \Leftrightarrow FeOH^-_{ads} \qquad \text{vs.} \qquad Fe + AlO_2^- \Leftrightarrow FeAlO^-_{2_{ads}}$$

* Slow strain rate testing measures loss of ductility or decrease in ultimate tensile strength as it is strained to failure while immersed in the corrosive solution. The test can be made further conservative by impressing an electrical potential within the active-passive transition regions determined by the anodic polarization testing. The threshold stress intensity required for CSCC can be measured by loading a modified compact tension specimen (‘wedge-opening loaded specimen) to a known stress intensity and exposing the specimen to the corrosive solution. The length of crack extension can then be determined through standardized methods.

In the active region of the curve at electrochemical potentials more active than the initial active passive transition peak, the oxide film is then a mixed iron oxide-iron aluminate formation, as opposed to the typical magnetite (Fe_3O_4).

Mixed iron oxide-iron aluminate: $Fe_{3-x}Al_xO_4$

However, the ability of this mixed oxide to maintain stability in the passive regions and consequent inhibiting effect on stress corrosion cracking is debatable. While the reaction chemistry indicates that the shifts in potential may create a region of anodic protection, crack propagation studies have indicated that the aluminate ion is detrimental to crack growth rates once initiated in hydroxide solutions.[15] This effect may be due to the instability of the oxide film and the repassivation kinetics, once disturbed. The initiation and propagation of stress corrosion cracking is a complex mechanism that includes the film rupture as well as repassivation kinetics. [16] Instability of an adherent oxide film by straining the material can promote the anodic dissolution processes typical of nitrate corrosion or caustic cracking.[17,18] The specific oxide film reported to be stable in concentrated solutions of hydroxide and nitrate is contradictory. The Fe_2O_3 film is thought to be more ductile than Fe_3O_4, thereby requiring higher stress intensities for rupture to maintain an exposed crack tip.[19] On the other hand, Fe_3O_4 is reported to be more protective against nitrate induced IGSCC by protecting grain boundaries from preferential dissolution.[20] The stability of oxide film and its ability to reform is considered to be the controlling factor in CSCC.

4 TECHNICAL APPROACH

The experimental test program, developed based upon previous test results and expected conditions during the current sludge mass reduction (SMR) campaign, consisted of electrochemical and mechanical testing to determine the susceptibility of ASTM A516 carbon steel to CSCC in the relevant environment. The electrochemical testing consisted of anodic polarization scans to determine electrochemical potential regimes in which CSCC was possible or inhibited. The mechanical testing consisted of exposing U-bend coupons to relevant chemistry and temperature regimes to determine propensity for cracking.

4.1 Electrochemical Testing: Anodic Polarization

Anodic polarization curves, which are plots of electrochemical potential as a function of current density, were measured to determine electrochemical potential regions or zones over which CSCC may occur. A schematic of an anodic polarization curve is shown in Figure 2, where the shaded zones (regions of transition between the passive and active states) indicate the electrochemical potentials required for SCC in susceptible alloy-solution combinations. In the transition regions, the passive films are unstable thus increasing susceptibility to SCC.

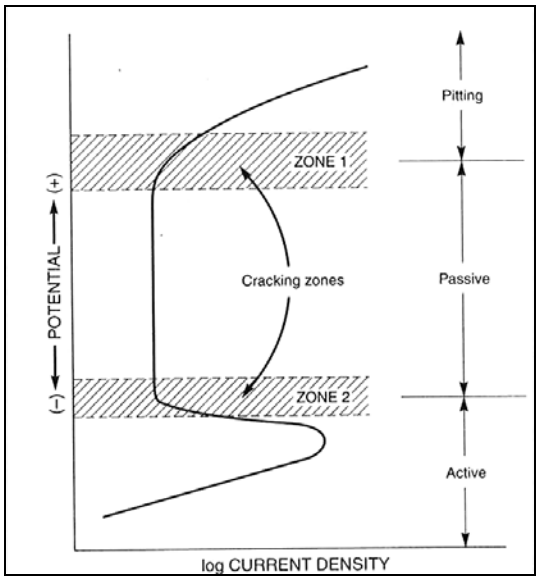

Figure 2: Schematic of Anodic Polarization Curve Showing Zones Susceptible to SCC [21]

The active passive transition region begins with an active corrosion region followed by a "peak current density" or the passivation potential, indicating instability in the oxide film. This is representative of a large current density changes over a small potential changes, which are indicative of SCC.

4.2 Matrix

The anodic polarization behavior of low carbon steel, ASTM A516-70, was determined in solutions with compositions expected during the sludge mass reduction campaign. Test matrix variables included hydroxide concentration (5, 10M), nitrate concentration (0-1M), aluminate concentration (0-1M) and temperature (95°C,105°C). The nominal composition of ASTM A516-70 low carbon steel is shown in Table 4, with test matrix variables summarized in Table 5.

Table 4: Nominal Composition of ASTM A516-70 Steel.

Elements	Nominal $(wt\%)_{max}$
C	$t \leq 0.5$in. 0.27 0.5in. $< t \leq 2$in. 0.28
Mn	0.85-1.2
P	0.035
S	0.035
Si	0.15 - 0.4

* Where t = thickness of plate

Table 5: Test Matrix Variables (Parametric Matrix)

NaOH [M]	$NaNO_3$ [M]	$NaAlO_2$ [M]	Temperature (C)
5	0.1	0.1	95
10	0.5	0.5	105
	1	1	

The anodic polarization scans were obtained using a computer-controlled potentiostat (EG&G PAR Model 273A). The tests were performed in a three-electrode one-liter cell made of Teflon© (PTFE) with use of heating tape to control temperature (± 2°C). The working electrode was encapsulated in a metallurgical epoxy mount. A graphite counter electrode was used in the solution. A Hg-HgO electrode encased in a PTFE body was used as the reference electrode. The anodic polarization scans were run at a scan rate of 0.5 mV/s, over a potential range of -1.1V vs. E_{ref} to 1.1 V vs. E_{ref}. The open circuit potential was measured for 2 hours prior to the anodic polarization scan.

4.3 Mechanical Testing

Mechanical testing to determine the susceptibility of low carbon steel to CSCC was performed by exposing U-bend coupons (shown in Figure 3) to the most concentrated solutions within the test matrix at 105°C, considered to be bounding conditions. U-bend testing was done by exposure of welded, highly stressed coupons for 35 days.

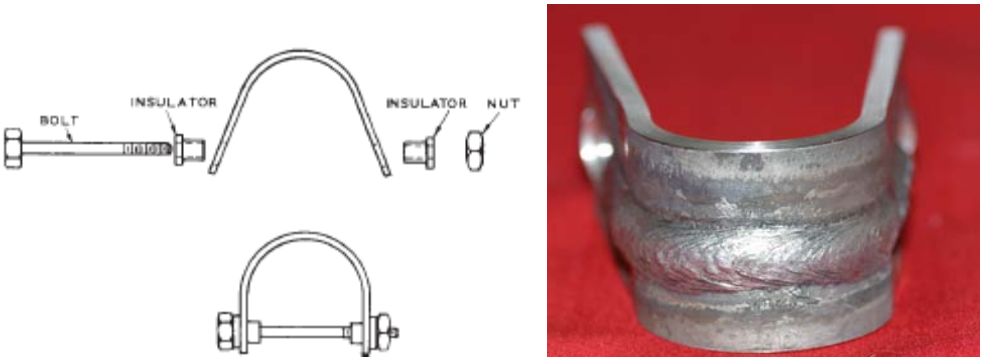

Figure 3: U-Bend Coupons

5 ELECTROCHEMICAL TEST RESULTS

The anodic polarization scans were analyzed to determine the electrochemical potential regions in which stress corrosion cracking is possible. The U-bend coupons were examined visually for evidence of cracking followed by dye-penetrant testing. The results of the anodic polarization scans and the U-bend testing are presented here, and used to recommend limits during the SMR campaign.

5.1 Anodic Polarization Scans: 5M/10M NaOH + $NaNO_3$

The results of the anodic polarization scans performed on low carbon steel exposed to 5M NaOH with various additions of only $NaNO_3$ are shown in Figure 4-5 for 95 and 105°C respectively. The anodic polarization scan for steel exposed to 10M NaOH with various additions of $NaNO_3$ for 95°C is shown in Figure 6. It is important to note that the testing performed for the 10M NaOH solution were performed at a beginning potential of -0.2V vs. E_{OC}, while all other testing were performed at a beginning potential of -1.1V vs. E_{ref}. The impacts of these testing parameters will be discussed.

The scan performed in the 5M NaOH (Figure 4-5) solution without any additions exhibited several distinct characteristics: (i) a short active dissolution regime, (ii) followed by a broad active to passive transition peak, (iii) a small second transition peak (iv) a passive region (v) a transpassive regime. The addition of 0.1M $NaNO_3$ to the solution resulted in the initial broad peak being divided into two peaks for both temperatures for the 5M solution, while E_{corr} remained similar to the initial solutions. However, there were discrepancies between the E_{OC} as measured prior to the polarization test and the E_{corr}.measured during the polarization scan. The scans performed in the 10M NaOH solution shifted E_{corr} into the upper regions of the initial broad peak. The solutions in which the beginning potentials were subject to significant cathodic currents essentially presenting NaOH to the surface of the working electrode during the test and simulating the same condition without inhibitors. However, the E_{OC} measured during the testing was used to determine the inhibitor effects . In spite of the testing technique, the addition of 0.5M $NaNO_3$ to 5M NaOH solution shifted E_{corr} into a region above the initial active-passive transition peak when tested at

95°C, but not at 105°C. The addition of 1M $NaNO_3$ returns the E_{corr} to the initial conditions with the broad active passive transition peak, but limits the peak current density indicating a greater stability of the oxide film.

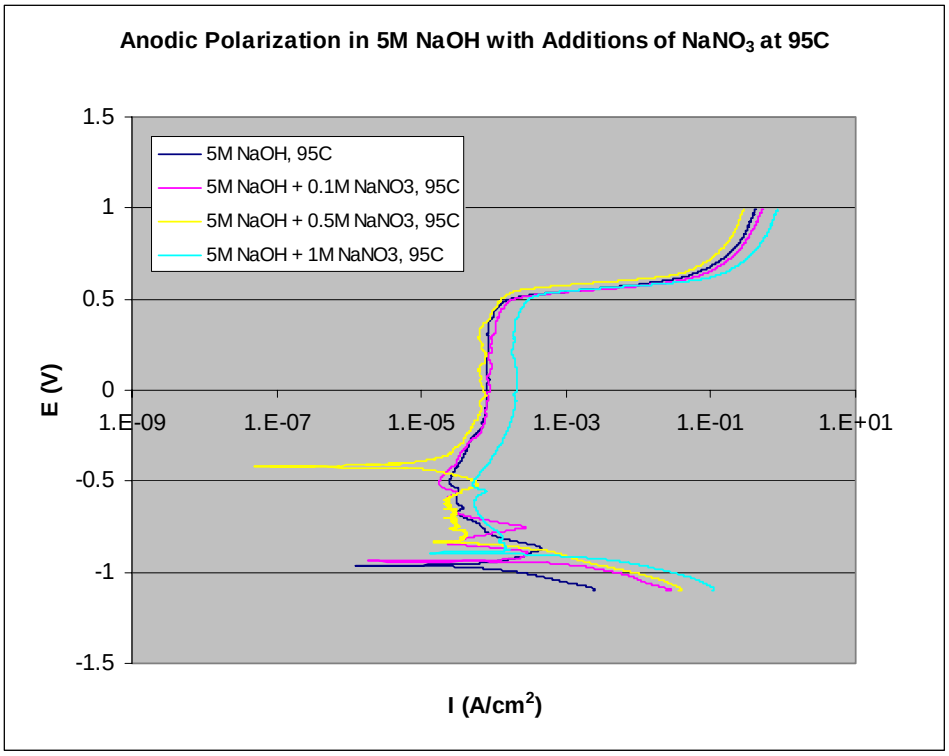

Figure 4: Anodic Polarization in 5M NaOH with Additions of $NaNO_3$ at 95C

The results of the anodic polarization scans performed on the 5M NaOH solutions with additions of $NaNO_3$ at 105°C were similar to the scans performed at 95°C with some important differences. The addition of 0.5M $NaNO_3$ did not shift the E_{corr} beyond the initial active transition peak, but exhibited results similar to that of the 0.1M $NaNO_3$ addition, i.e. initial broad active passive transition peak devolved into two sharp peaks. The addition of the 1M $NaNO_3$ test at 105°C shifted the E_{corr} into the upper region of the active passive transition peak and limited the broad peak current density similar to that of the test in the 10M solutions with less addition of $NaNO_3$, as shown in Figure 6.

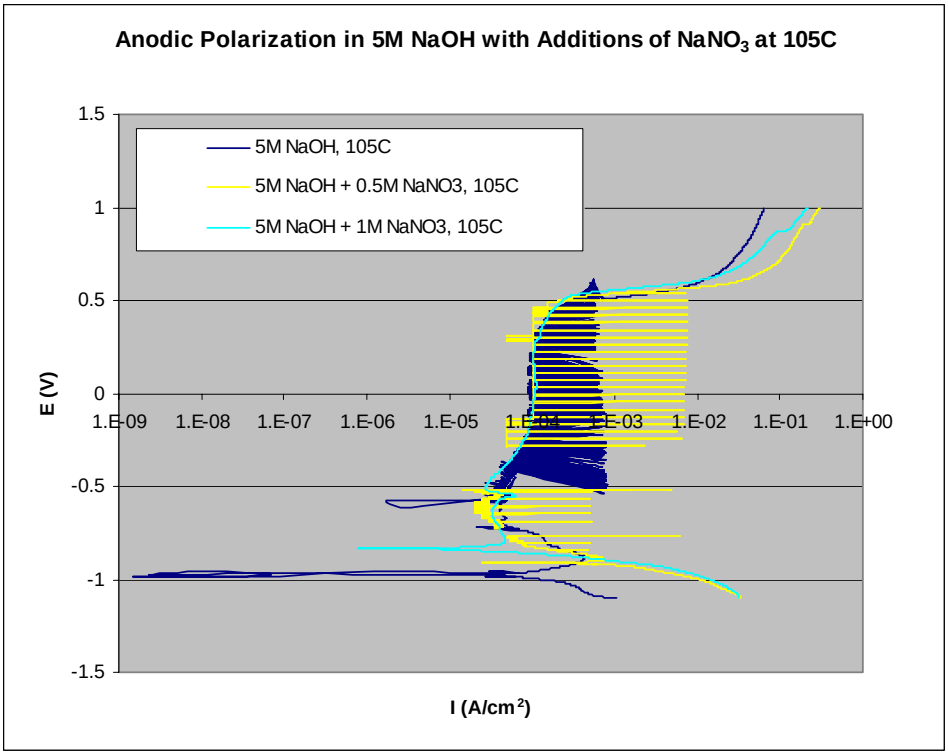

Figure 5:Anodic Polarization in 5M NaOH with Additions of $NaNO_3$ at 105C

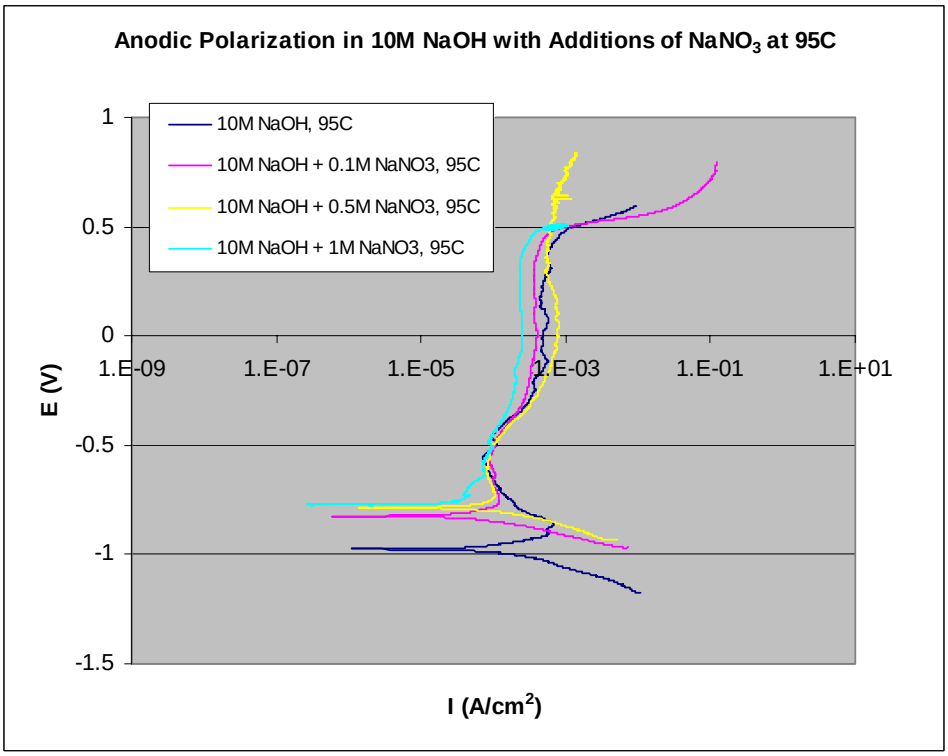

Figure 6: Anodic Polarization in 5M NaOH with Additions of $NaNO_3$ at 95°C

5.2 Anodic Polarization Scans: 5M/10M NaOH + 0.1MNaNO$_3$ + NaAlO$_2$

The anodic polarization scans for steel exposed to 5M NaOH with 0.1M $NaNO_3$ and varying levels of $NaAlO_2$ additions are shown in Figure 7 - 8 for 95 and 105°C respectively. The scans at 95°C show that increasing aluminate concentration broadens the active-passive transition peak effectively eliminating the second peak. The scans at 105°C show that aluminate still sharpens the initial active region, but no longer broadens the initial active passive transition peak. However, the second active passive transition peak is eliminated with increasing aluminate concentration.

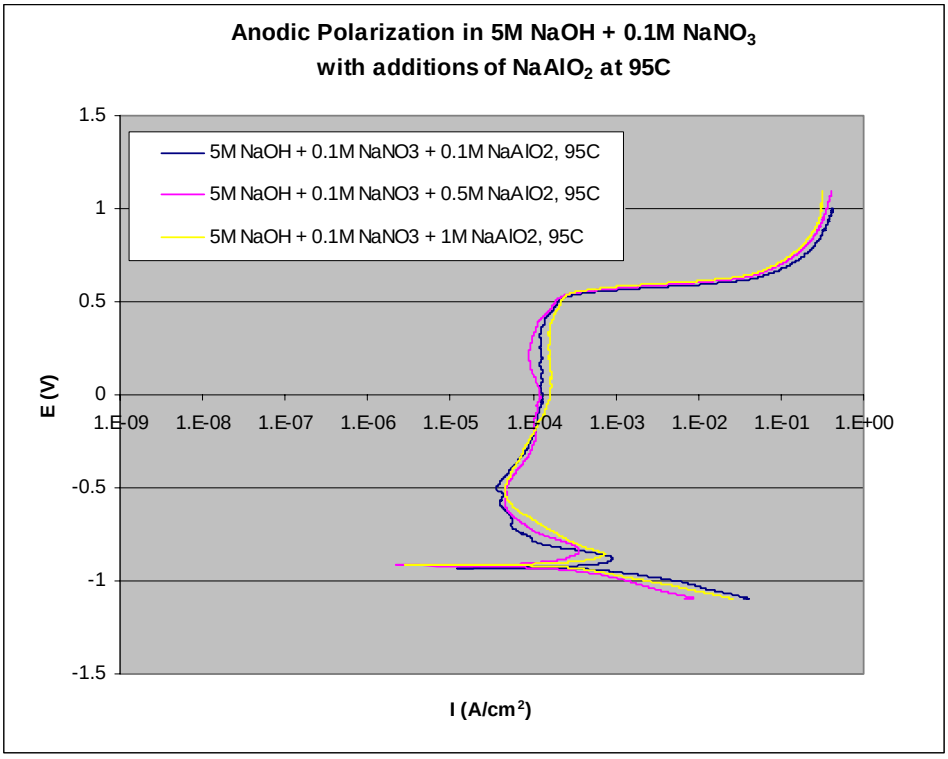

Figure 7: Anodic Polarization Scan in 5M NaOH with 0.1M $NaNO_3$ and additions of $NaAlO_2$ at 95°C

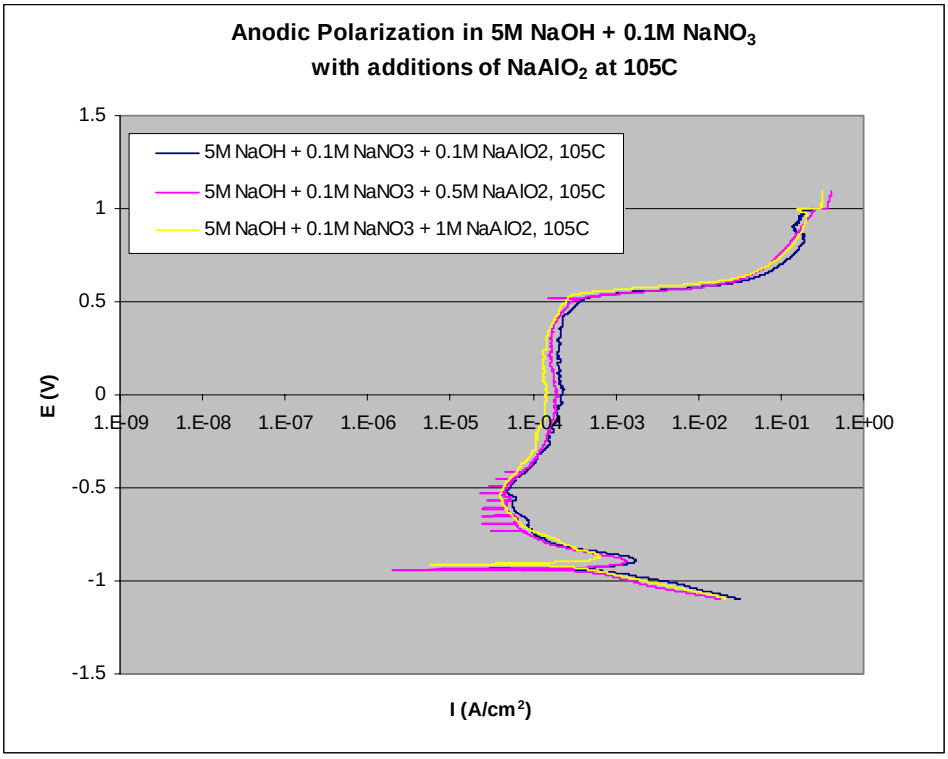

Figure 8: Anodic Polarization Scan in 5M NaOH with 0.1M $NaNO_3$ and additions of $NaAlO_2$ at 105°C

The anodic polarization scans for steel exposed to 10M NaOH with 0.1M $NaNO_3$ and varying levels of $NaAlO_2$ additions are shown in Figure 9 - 10 for 95 and 105°C respectively. The initial active region has become very sharp with 10M NaOH at 95°C and the broad initial active transition peak has devolved into two smaller peaks. In this case with the increased hydroxide concentration, the aluminate does not suppress any of the transition peaks as with the 5M NaOH solution with 0.1M $NaNO_3$ addition. The scans taken at 105°C indicate that with only 0.1M $NaAlO_2$ concentration, the E_{corr} is shifted beyond the active passive transition region, in spite of the test technique. However, with increasing aluminate concentration, the E_{corr} returns to potentials where the transition peaks are present. This is consistent with previous findings that with increasing ionic strength, the dissolved oxygen content and consequently the ability to form a stable oxide film is diminished.

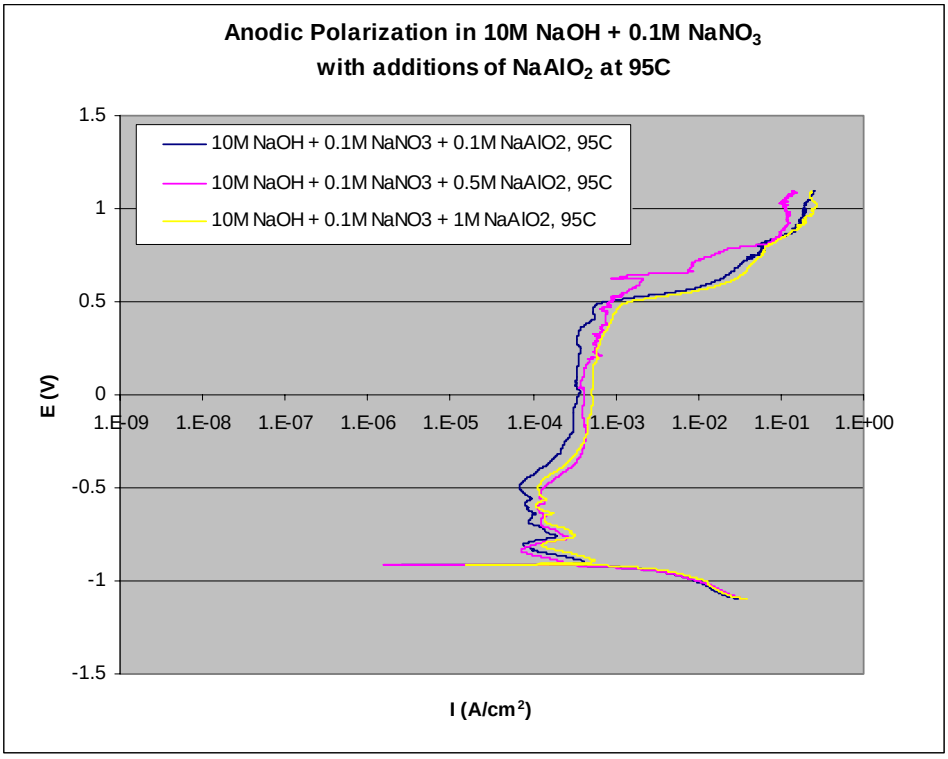

Figure 9:Anodic Polarization Scan in 10M NaOH with 0.1M $NaNO_3$ and additions of $NaAlO_2$ at 95°C

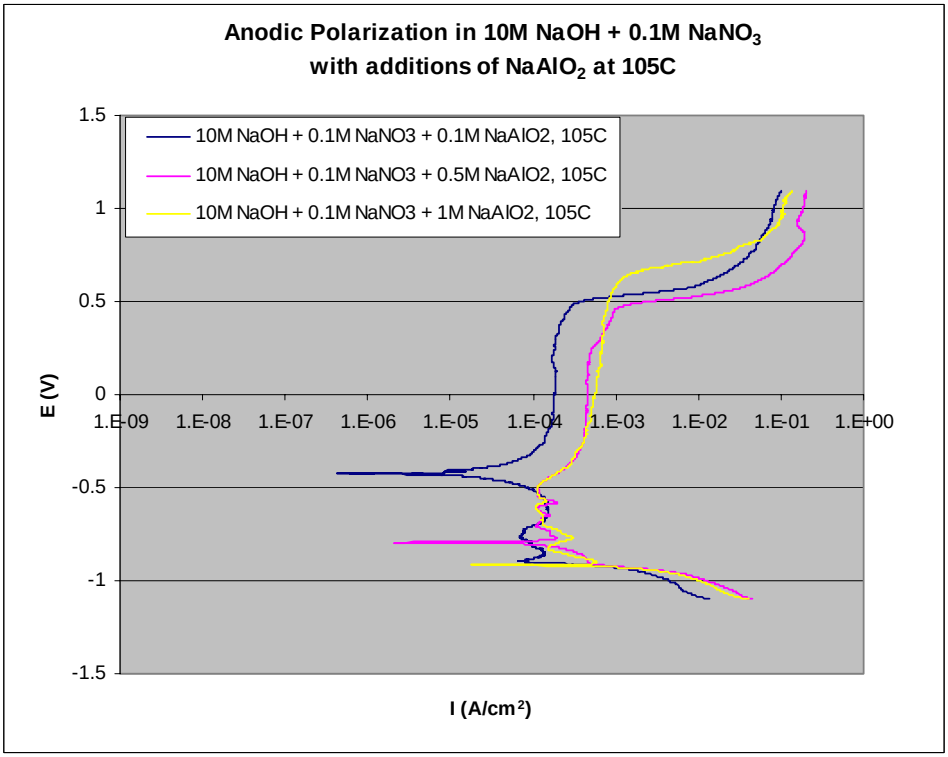

Figure 10: Anodic Polarization Scan in 10M NaOH with 0.1M $NaNO_3$ and additions of $NaAlO_2$ at 105°C

5.3 Anodic Polarization Scans: 5M/10M NaOH + 0.5MNaNO$_3$ + NaAlO$_2$

The addition of 0.5M $NaNO_3$ to 5 and 10M NaOH solutions is known to shift E_{corr} into electrochemical potential regimes where the initial active passive transition peak is bypassed thereby inhibiting against CSCC. However, the addition of aluminate will affect this anodic inhibition against CSCC. The anodic polarization scans for steel exposed to 5M NaOH with 0.5M $NaNO_3$ and varying levels of $NaAlO_2$ additions are shown in Figure 11 - 12 for 95 and 105°C respectively. The scans performed at 95°C indicate broadening of the initial active transition peak with increasing aluminate concentration, with the associated elimination of the second peak. However, the E_{corr} has not shifted, most likely to the extreme cathodic polarization, which will be resolved with the analysis of the E_{OC}. However, there is evidence that the aluminate is passivating the surface due to the limiting of the current density beyond the peak.

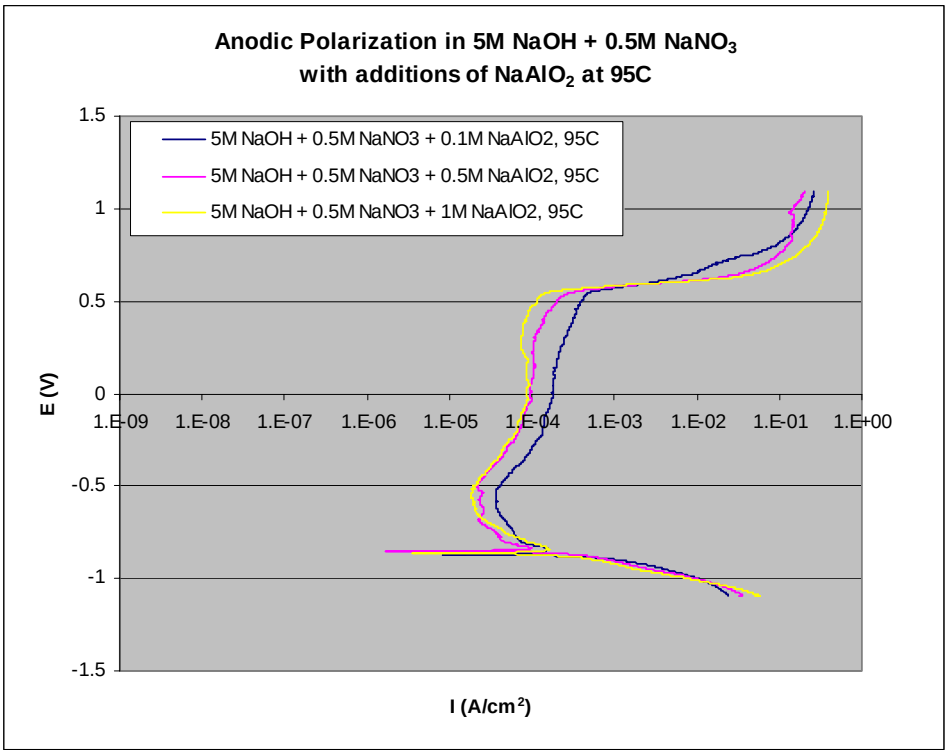

Figure 11: Anodic Polarization Scan in 5M NaOH with 0.5M $NaNO_3$ and additions of $NaAlO_2$ at 95°C

The scans performed at 105°C indicated a shift in the E_{corr} beyond the initial active passive transition peak when 0.5M $NaAlO_2$ was added, while the smaller and larger additions did not of shift the E_{corr}. However, with additions of 0.1M and 1M $NaAlO_2$, there appears to be a limiting current density at the electrochemical potentials of the initial active passive transition peak, or a truncation of the peak. In fact, all three tests indicate a limiting current density in this regime.

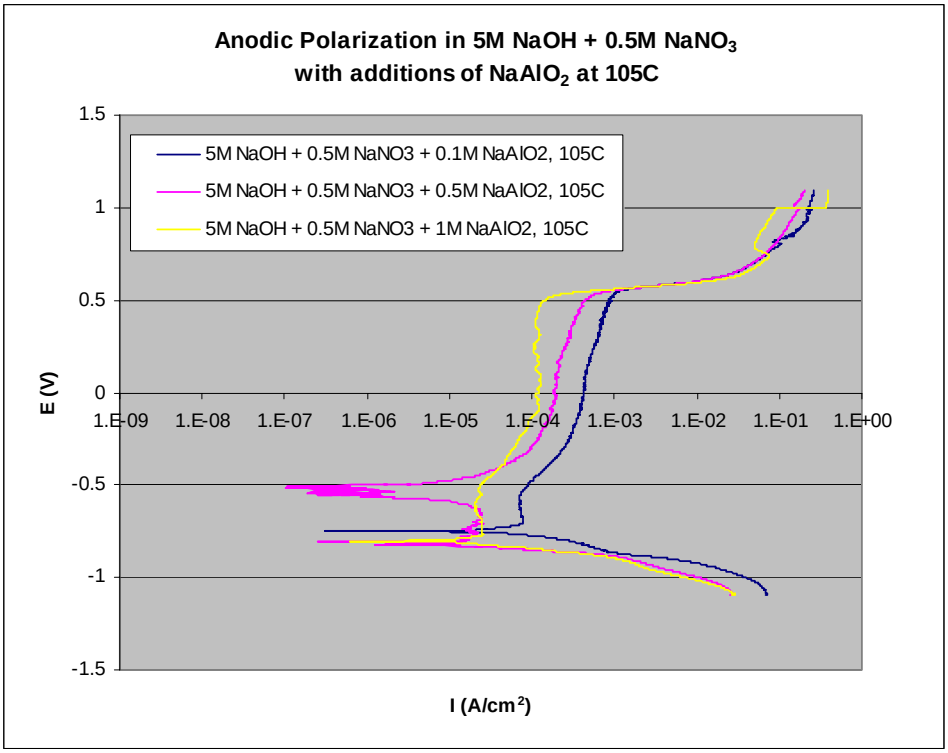

Figure 12: Anodic Polarization Scan in 5M NaOH with 0.5M $NaNO_3$ and additions of $NaAlO_2$ at 105°C

The anodic polarization scans for steel exposed to 10M NaOH with 0.5M $NaNO_3$ and varying levels of $NaAlO_2$ additions are shown in Figure 13 - 14 for 95 and 105°C respectively. The scans at 95°C indicate that the initial active passive transition peak is nearly eliminated/truncated with decreasing aluminate concentration. In general, the addition of 0.5M $NaNO_3$ has shifted the E_{corr} to more active potentials, limiting the peak current density and the electrochemical potential of the active passive transition peaks. The test results at 105°C also indicate similar trends, with the peak being nearly eliminated with increasing aluminate concentration.

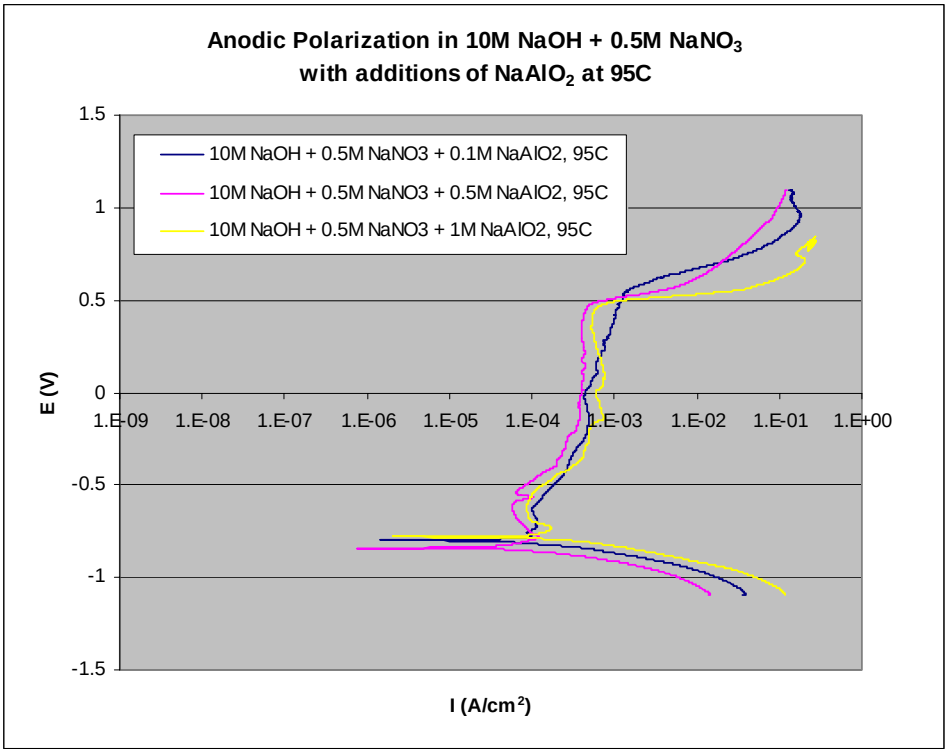

Figure 13: Anodic Polarization Scan in 10M NaOH with 0.5M $NaNO_3$ and additions of $NaAlO_2$ at 95°C

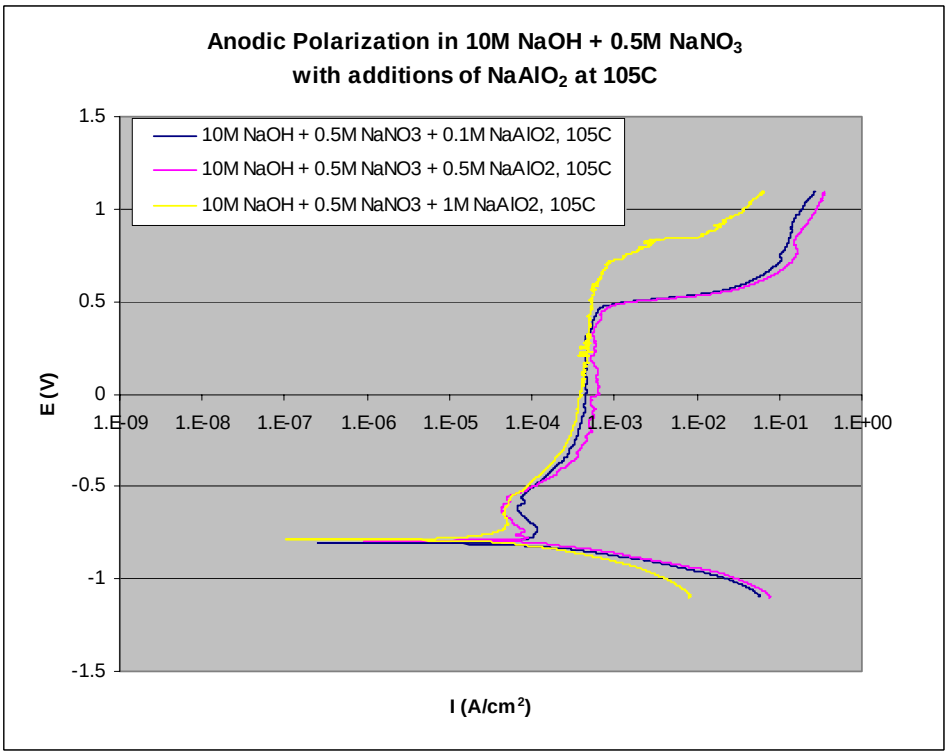

Figure 14: Anodic Polarization Scan in 10M NaOH with 0.5M $NaNO_3$ and additions of $NaAlO_2$ at 105°C

5.4 Anodic Polarization Scans: 5M/10M NaOH +1.0M$NaNO_3$ + $NaAlO_2$

The addition of 1M $NaNO_3$ to 5 and 10M NaOH solutions is also known to shift E_{corr} into electrochemical potential regimes where the initial active passive transition peak is bypassed at lower temperatures, but not as inhibiting in the temperatures tested here. However, in some cases, the addition of nitrate/aluminate appears to have sufficiently shifted E_{corr} beyond the initial active passive transition peak.

The anodic polarization scans for steel exposed to 5M NaOH with 1M $NaNO_3$ and varying levels of $NaAlO_2$ additions are shown in Figure 15 - 16 for 95 and 105°C respectively. The Ecorr appeared to shift to more active values with increasing aluminate content for the scans performed at 95°C, but the peak current density was limited even in the more noble regions. However, the E_{corr} was shifted to more noble potential for each of the conditions. The scans performed at 105°C indicated a shift of E_{corr} to more noble potentials than the initial active passive transition peak for additions of 0.1M and 1M aluminate, but at 0.5M additions did not shift the E_{corr}.

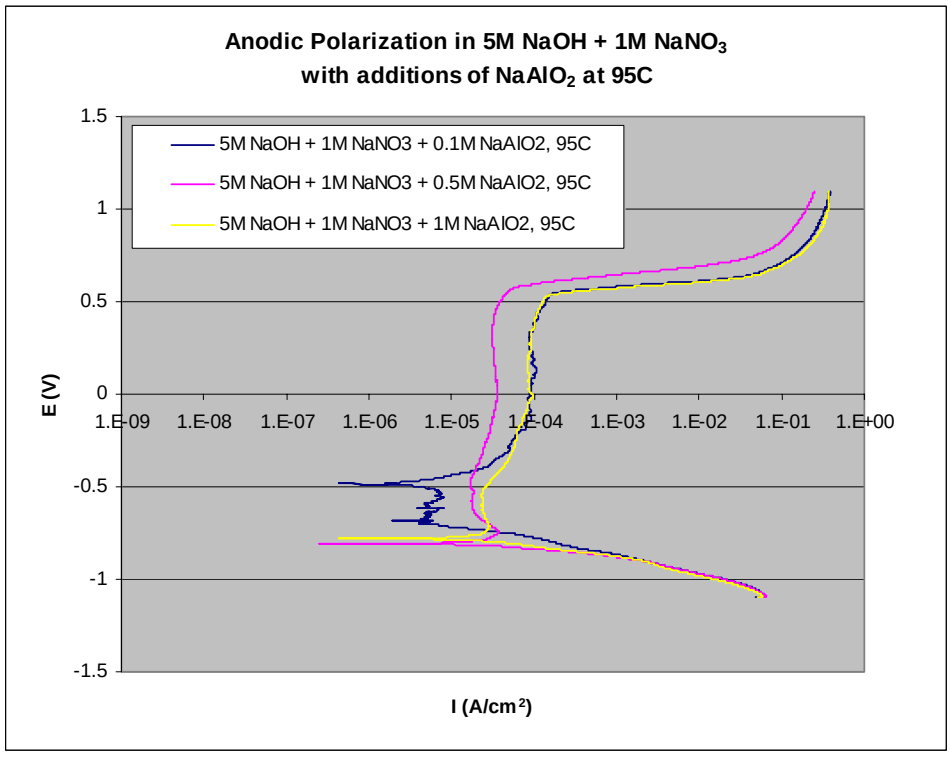

Figure 15: Anodic Polarization Scan in 5M NaOH with 1M $NaNO_3$ and additions of $NaAlO_2$ at 95°C

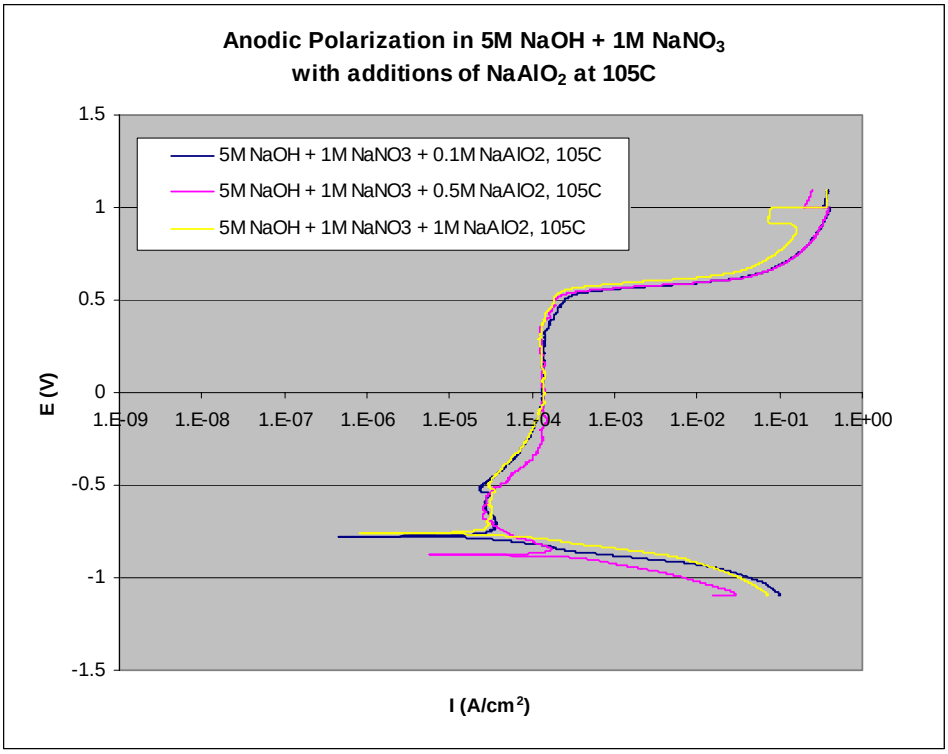

Figure 16: Anodic Polarization Scan in 5M NaOH with 1M $NaNO_3$ and additions of $NaAlO_2$ at 105°C

The anodic polarization scans for steel exposed to 10M NaOH with 1M $NaNO_3$ and varying levels of $NaAlO_2$ additions are shown in Figure 17 - 18 for 95 and 105°C respectively. The scans in the most concentrated of these solutions indicated a shift of E_{corr} beyond the initial active passive transition peak, or a limit in the peak current density in this region of potentials with increasing aluminate contents.

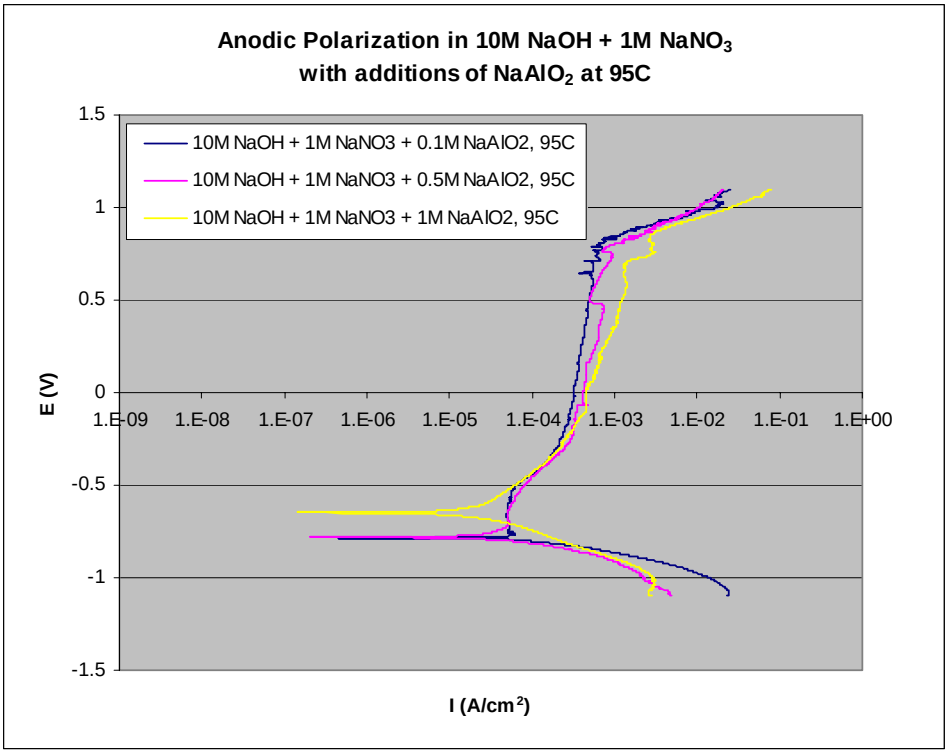

Figure 17: Anodic Polarization Scan in 10M NaOH with 1M $NaNO_3$ and additions of $NaAlO_2$ at 95°C

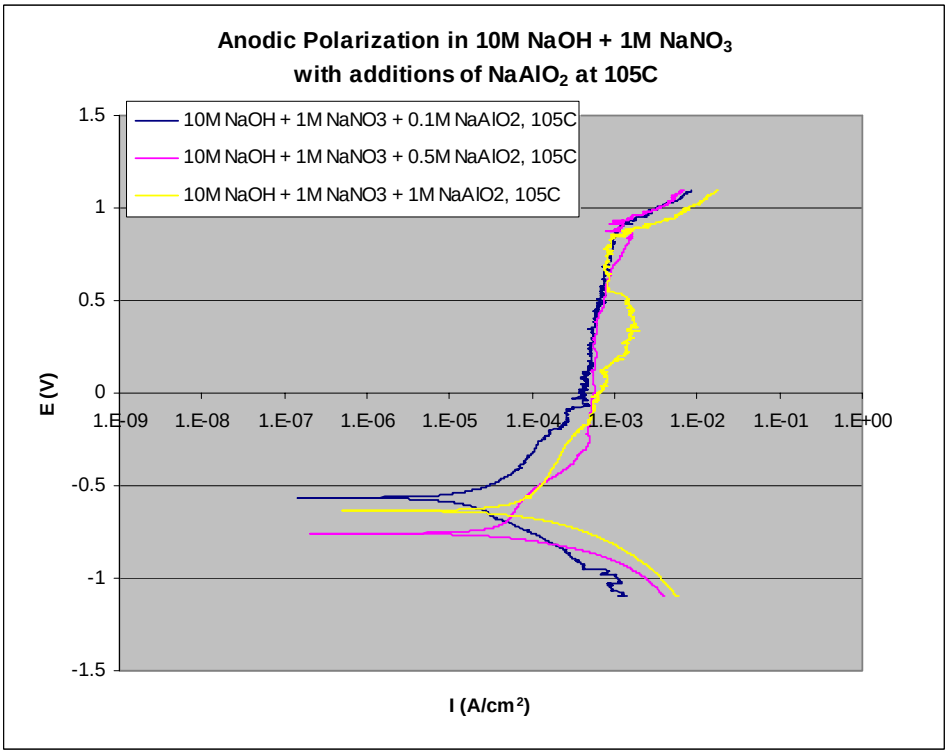

Figure 18:Anodic Polarization Scan in 10M NaOH with 1M $NaNO_3$ and additions of $NaAlO_2$ at 105°C

6 ELECTROCHEMICAL TEST DISCUSSION

The results revealed several key characteristics of the anodic polarization behavior of low carbon steel in mixed sodium hydroxide, sodium nitrate, and sodium aluminate environments. Low carbon steel undergoes several oxidation stages during anodic polarization in these highly concentrated solutions. The effect of nitrate on the oxidation is a component in controlling the suppression of active-passive transition peaks that correlate to electrochemical potential regimes where SCC may occur. The addition of aluminate ions to the solutions also greatly impacts the electrochemical behavior, most probably due to inclusion into the oxide film creating a mixed iron oxide/aluminate passive film.

The oxides associated with active-passive transition peaks in concentrated NaOH solutions were identified through x-ray diffraction techniques. [22] The first active-passive transition peak, observed in this study at -0.9V to -0.55 V-HgO, corresponded to the dissolution of iron as $HFeO_2^-$ with the ultimate formation of a Fe_3O_4 film, as indicated by the Pourbaix diagram. The intermediate steps include the formation of $Fe(OH)_2$, which breaks down to form Fe_3O_4. The second, small, active-passive transition peak seen in this study at -0.45V-HgO for the 10M NaOH solution corresponded to the further oxidation of Fe_3O_4 to Fe_2O_3. These results are also in accordance with the literature results of comparing anodic polarization scans with theoretical thermodynamic considerations.[10-12] They concluded that the hydroxyl ion plays the key role by accelerating iron dissolution at active potentials and promoting dissolution of Fe_2O_3 film.

The anodic polarization scans revealed that with various additions of a sodium nitrate, a strong oxidizer, the active-passive transition peaks were suppressed. The cathodic depolarization by nitrate causes the E_{corr} to shift to more passive values than in the presence of oxygen alone, thereby preventing SCC. The suppression of the active peaks results from an increase in the cathodic polarization current corresponding to the depolarization of the cathodic reaction by the strong oxidizers. Therefore carbon steel is polarized to more positive potentials where Fe_2O_3 is stable. However, this type of "anodic protection" methodology must be applied judiciously due to the possibility of localized shifts in the open circuit potential due to localized chemistry changes.

The E_{OC} is driven beyond the active-passive transition only for addition of 0.5M $NaNO_3$ at 95°C, as shown in Figure 19 . At lower levels of nitrate additions, E_{corr} is not sufficiently affected to suppress the initial active-passive transition peak. The E_{OC} is polarized above the initial peak with additional sodium nitrate additions, but returns to more active potentials at a concentration of 1M $NaNO_3$, and remains low at higher temperatures in this critical region.

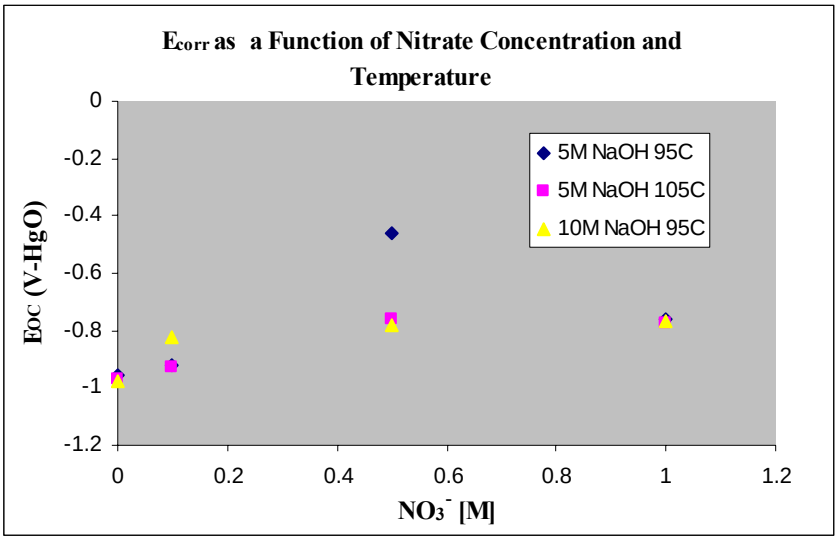

Figure 19: Effect of $NaNO_3$ addition to NaOH solutions on E_{OC}.

The effect of aluminate addition to the nitrate/hydroxide solutions was analyzed utilizing the 2-hour open circuit potential data, since E_{corr} was measured subsequent to the large cathodic charging. The addition of aluminate in the

solutions containing only 0.1 M $NaNO_3$ is shown in Figure 20. The data is consistent with previous testing that showed that E_{OC} is insufficiently shifted into anodic regions to bypass the initial transition peak. The aluminate additions though, appear to shift the E_{OC} into more anodic potentials limiting the peak current density. Only the addition of 0.1M $NaAlO_2$ to the 10M solution showed a sufficient anodic shift in the E_{corr} when tested at 105°C.

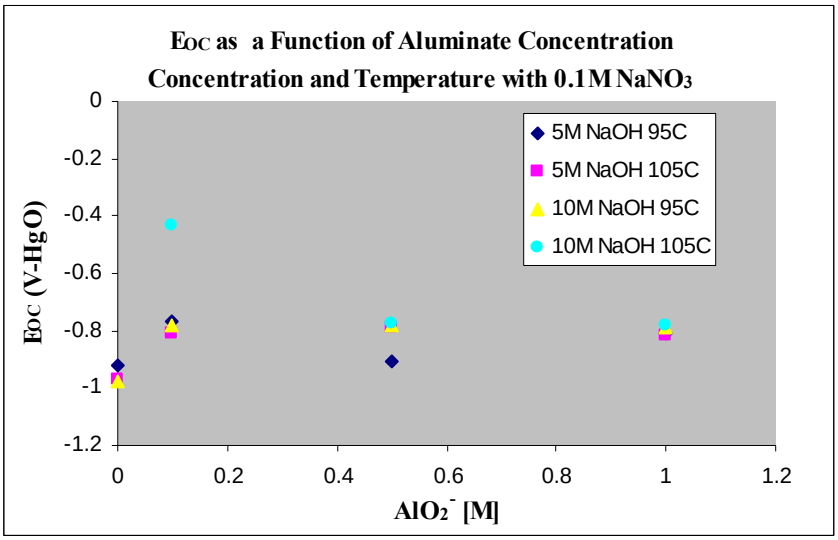

Figure 20: E_{OC} as a Function of Aluminate in 0.1M NaNO3/NaOH Solutions

The addition of aluminate in the solutions containing only 0.5M $NaNO_3$ is shown in Figure 21. The addition of 0.5M $NaNO_3$ is typically the most inhibited solutions, however, previous testing indicated that the minimization of oxygen concentration as ionic strength increased tended to decrease oxide film stability. The addition of aluminate to these solutions is sufficient to shift E_{OC} beyond the initial active-passive transition peak only in specific cases, e.g. 95C with 1M addition of aluminate.

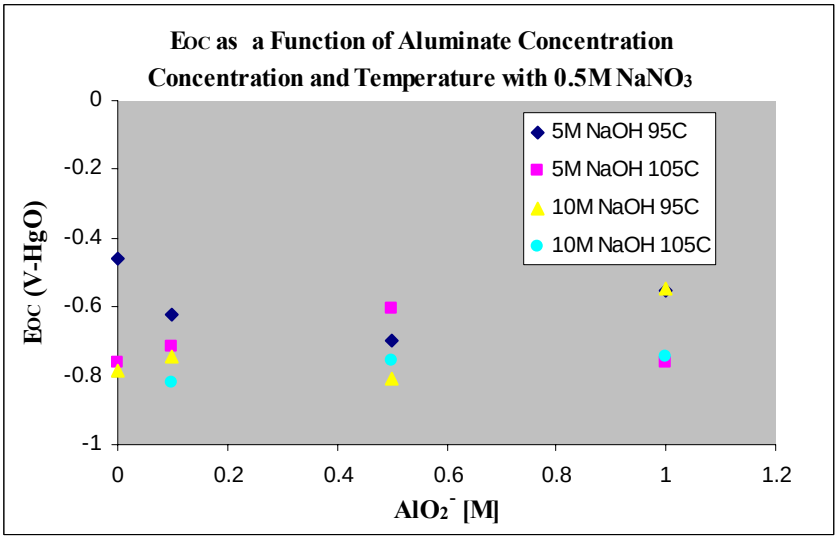

Figure 21: E_{OC} as a function of Aluminate in 0.5M $NaNO_3$/NaOH Solutions.

The addition of aluminate in the solutions containing only 1M $NaNO_3$ is shown in Figure 22. The addition of 1M $NaNO_3$ to NaOH is known to anodically inhibit again CSCC at lower temperatures, but not at higher temperatures. In this case, the data suggest that addition of aluminate appears to aid in the anodic shift of the E_{OC} in specific cases.

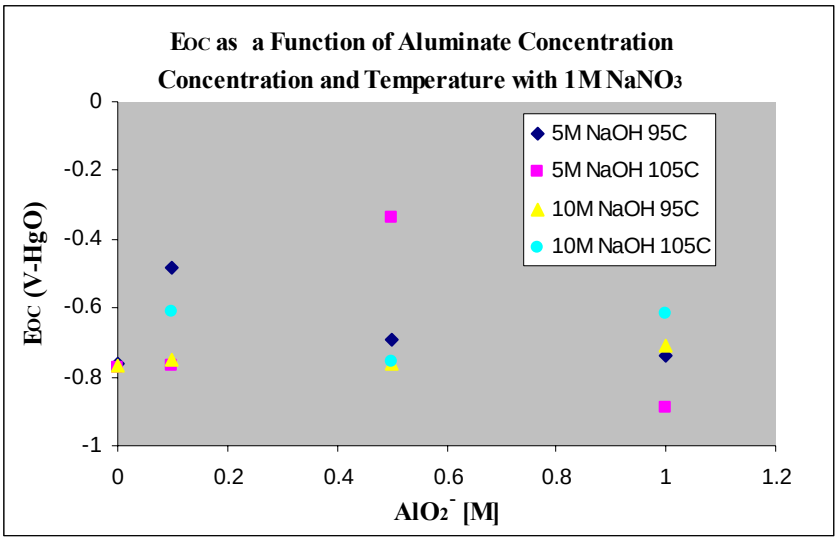

Figure 22: E_{OC} as a function of Aluminate in 1M $NaNO_3$/NaOH Solutions

The analysis of the electrochemical data revealed that there is no consistent anodic shift of the E_{OC} to conclusively claim anodic protection from CSCC, although there are specific cases where the anodic shift if sufficient. In addition, the cathodic charging of the system prior to the anodic polarization, led to a large variance between E_{OC} and E_{corr} indicating the propensity for localized chemistry changes playing a major role on the electrochemical potentials. As such, it was concluded that anodic protection from CSCC in these conditions is not consistently applicable. Therefore, mechanical testing in the form of U-bend testing was performed to determine whether cracking can be initiated under relevant conditions.

7 RESULTS OF MECHANICAL TESTING

Mechanical testing in the form of U-bend testing was performed in the most concentrated solutions at temperatures of 105C. The U-bend coupons were fabricated through laser cutting of butt-welded low carbon steel plate conforming to ASTM A537-Cl.1 standards. The plates were butt welded transverse to the rolling direction of the plate using a shielded metal arc procedure with E7018 H4R welding electrodes. Coupons were then laser cut from the plate with the weld in the long transverse-longitudinal orientation and centered with respect to the transverse direction or width; coupon size was 5 in long, 1.5 in wide and 0.375 in thick. Samples were configured in this orientation so crack propagation would occur in the longitudinal rolling direction. Only the edges were ground to remove any burrs. The coupons were bent around a mandrel with radius of 0.505 in. The U-bends were received with mill oxide layers on both inside and outside surfaces. Each sample was stenciled with a unique number and the material grade. U-bends were made following G30-97, "Making and Using U-bend Stress-Corrosion Test Specimens".

The welds in the U-bends were in the longitudinal direction to simulate the residual stress fields of the fabrication welds in the waste tanks. Analyses of the welding process concluded that residual stresses in the tanks through the fabrication process were greater perpendicular to the welds.[23] This data is further corroborated by the known history of nitrate induced cracking in the Type I/II tanks which are perpendicular to fabrication welds.[†]

The exposure of the U-bend coupons was performed in Teflon containers within an oven as shown in Figure 23. The coupons were stressed using a torque wrench until the sides were parallel. The stainless steel load bolt was electrically insulated from the coupon with Teflon washers.

[†] Stress corrosion cracking in the Type II tanks that have a curved morphology are known to be due to the interaction of residual stress fields between repair welds and fabrication welds in close proximity.

Figure 23: U-Bend Coupons in Test

Once the exposures of 35 days were complete, dye penetrant testing was used to detect the presence of surface cracks. The dye penetrant testing revealed no cracking in any of the coupons after nominally 35 days of exposure, as shown in Table 6.

Table 6: Results of Dye Penetrant Testing

NaOH	$NaNO_3$	$NaAlO_2$	Results of Dye Penetrant Testing
5	0.1	0.1	
5	0.1	0.5	
5	0.1	1	

NaOH	$NaNO_3$	$NaAlO_2$	Results of Dye Penetrant Testing
5	0.5	0.1	
5	0.5	0.5	
5	0.5	1	
5	1	0.1	
5	1	0.5	
5	1	1	
10	0.1	0.1	

NaOH	$NaNO_3$	$NaAlO_2$	Results of Dye Penetrant Testing
10	0.1	0.5	
10	0.1	1	
10	0.5	0.1	
10	0.5	0.5	
10	0.5	1	
10	1	0.1	

NaOH	$NaNO_3$	$NaAlO_2$	Results of Dye Penetrant Testing
10	1	0.5	
10	1	1	

The U-bend testing performed here represents a highly aggressive mechanical conditions that is considered bounding for the Type III/IIIA high level waste tanks. These tanks have undergone a post-weld heat treatment stress relief process that precludes the initiation of stress corrosion cracking.

8 CONCLUSION

The temperature limits outlined by the chemistry control program for high level waste tanks for high hydroxide solutions will be exceeded during sludge mass reduction. Corrosion testing was performed to determine the potential for caustic stress corrosion cracking (CSCC) under expected conditions. The experimental test program, developed based upon previous test results and expected conditions during the current sludge mass reduction campaign, consisted of electrochemical and mechanical testing to determine the susceptibility of ASTM A516 carbon steel to CSCC in the relevant environment. Anodic polarization test results indicated that anodic inhibition at the temperatures and concentrations of interest for SMR is not a viable, consistent technical basis for preventing CSCC. However, the mechanical testing concluded that CSCC will not occur under conditions expected during SMR for a minimum of 35 days.

The envelope for corrosion control is recommended during the SMR campaign is shown in Table 7. The underlying assumption is that solution time-in-tank is limited to the SMR campaign. The envelope recommends nitrate/aluminate intervals for discrete intervals of hydroxide concentrations, although it is recognized that a continuous interval may be developed. The limits also sets temperature limits.

Table 7: Recommended Chemistry Control Envelope During Sludge Mass Reduction

Hydroxide Concentration (M)	Nitrate Concentration (M)	Aluminate Concentration (M)	Temperature (°C)
$[OH^-] < 5$	$0.2 < [NO_3^-] \leq 1$	$[AlO_2^-] \leq 1$	105°C
$5 \leq [OH^-] \leq 10$	$0.5 < [NO_3^-] \leq 1$	$[AlO_2^-] \leq 1$	105°C

Further U-bend testing is recommended under polarized conditions to determine whether the mechanical conditions exist for SCC when the test is electrochemical biased towards initiating CSCC.

REFERENCES

[1] NACE Corrosion Data Survey, 5th Edition, 1971.

[2] L.F. Fox, "CSTF Corrosion Control Program, Program Description Document," WSRC-IM-2003-00010, Rev.3, Westinghouse Savannah River Company, November 2004.

[3] J.E. Reihnohl, W.E. Berry, *Corrosion* 28 (1972), 151.

[4] R.N. Parkins, in: R.W. Staehle, J.Hochmann, R.D. McCright, and J.E. Slater (Ed.s), *Stress Corrosion Cracking and Hydrogen Embrittlement of Iron Base Alloys*, NACE, Houston, 1977, 601-619.

[5] K. Bohkenkamp, *Proc. Conf. Fund. Asp. of Stress Corrosion Cracking*, NACE, Columbus, 1967, 374.

[6] T.P. Hoar, R.W. Jones, *Corr. Sci.* 13 (1973) 725.

[7] M.J. Humphries, R.N. Parkins, *Corr. Sci.* 7 (1967) 747.

[8] W.C. Schroder, A.A. Berk, R.A. O'Brien, *Metals and Alloys* 8 (1937) 320.

[9] J.D. Fritz to: J.R. Wiley, "Control of Stress Corrosion Cracking During DWPF in-tank Alumina Dissolution Processing, DPST-88-252, E.I. Dupont de Nemours and Co., January 1988.

[10] J.D. Fritz to: J.R. Wiley, "Susceptibility of Waste Tanks to Stress Corrosion Cracking from DWPF in-tank Alumina Dissolution," DPST-88-310, E.I. Dupont de Nemours and Co., February 1988.

[11] K.H. Subramanian, J.I. Mickalonis, "Anodic Polarization Behavior of Low Carbon Steel in Concentrated Sodium Hydroxide Solution with Sodium Nitrate Additions (U)," WSRC-2004-00292," Westinghouse Savannah River Company, June 2004.

[12] K.H. Subramanian, J.I. Mickalonis, "Slow Strain Rate Testing of Low Carbon Steel in Concentrated Sodium Hydroxide Solutions with Nitrate Additions (U)," WSRC-2005-00156," Westinghouse Savannah River Company, April 2005.

[13] K.H. Subramanian to: D.J. Martin, "Chemistry Control Recommendations for Tanks with Nitrate Concentrations less than 1M," SRNL-MTS-2005-50010, May 2005.

[14] R. Sriram, D. Tromans, *Corr. Sci* 25 (1985) 79.

[15] H.H. Le, E. Ghali, *Corr. Sci.* 35 (1993) 432.

[16] D.A. Vermilyea, "Stress Corrosion Cracking and Hydrogen Embrittlement of Iron Base Alloys," NACE, (1977).

[17] T. P. Hoar, J. R. Galvele, *Corr. Sci* 10 (1970) 211.

[18] R. N. Parkins, *Corr. Sci*, 20 (1980) 147.

[19] R.B. Diegle, D.A. Vermilyea, *J. Electrocm. Soc.*, 122 (1975) 180.

[20] J. Flis, *Corr. Sci.*, 15 (1975) 553.

[21] Jones, D. A., Principles and Prevention of Corrosion, 2nd Ed., Prentice Hall, 1996.

[22] A.J. Salkind, C.J. Venuto, *J. Electrochem. Soc.* 111 (1964) 493.

[23] P. Dong, J. Zhang, et. al., “Task 1: Residual Stresses and Stress Intensity Factors for Single Butt Welds,” Final Report No. G003824-01, Battelle Memorial Institute, Columbus, OH 43201, September 1999.